Riemannian geometry-based detection of slow cortical potentials during movement preparation

Frigyes Samuel Racz[1,2], Rawan Fakhreddine[2], Satyam Kumar[2] and José del R. Millán[1,2]

***Abstract*— Slow cortical potentials - such as the readiness potential (RP) and the contingent negative variation (CNV) - provide means for controlling a brain-machine interface (BMI). RP and CNV precede self-paced and cued movements, respectively, and thus can be exploited for a variety of purposes such as robotic exoskeleton control or motor rehabilitation via BMI training. Single-trial detection of these patterns, however, is a challenging and therefore not yet fully resolved task, especially for online applications. Here we propose and evaluate a novel decoding algorithm for this cause, utilizing Riemannian geometry, template matching and adaptive re-centering for robust performance. We recruited 12 young, healthy volunteers who performed a center-out reaching task designed to evoke both RP and CNV in a sequential manner, while their neural activity was recorded using electroencephalography. Separate decoders of the same basic architecture were trained to detect RP and CNV on a single-trial basis, and data was evaluated offline on the subject level. RPs could be identified with a group average accuracy of 62.64±4.75% (ranging from 51.12% to 68.31%) with all but one subject surpassing chance levels, while CNVs were detected with an average accuracy of 74.01±7.49% (ranging from 62.24% to 85.00%) with all participants surpassing chance level. Even though evaluation was carried out offline, the proposed pipeline is readily adaptable to an online setting. Therefore, our Riemannian geometry-based approach show potential in single-trial detection of slow cortical potentials.**

***Clinical relevance*— Robust detection of RP and CNV and longitudinal BMI training could improve robotic control and neurorehabilitation.**

I. INTRODUCTION

Single-trial detection of electroencephalography (EEG) slow cortical potentials, such as the readiness potential (RP) or the contingent negative variation (CNV) preceding self-paced [1] or cued [2] movements, respectively, is still a challenging task. These neural patterns signal movement intent and/or preparation for motor execution, and therefore —if reliably identified— they can be exploited for a variety of purposes, such as improved robotic exoskeleton control [3], neurofeedback training [4] or other brain-machine interface (BMI) applications [5]. Many of the previously proposed solutions for this task rely on template matching, where detection of the pattern is confirmed if correlation of the collected neural data with a pre-defined (obtained or simulated) template surpasses a certain threshold [6]–[8]. Other attempts utilized more data-driven approaches, mostly using EEG signal amplitudes as features in their detection pipeline [5], [9]. Furthermore, multiple previous studies utilized pre-processing steps —such as independent component analysis (ICA)— that might raise concerns for online applications. For example, using ICA decomposition to remove artifactual components from neural signals online assumes that the obtained mixing matrix is stationary over time, however this is not necessarily the case. Therefore, consistent long-term performance of the decoder can only be expected if the obtained model parameters indeed remain constant over time, or the system is regularly re-calibrated.

In this work, we propose a novel decoding method that alleviates some of these shortcomings. Our method utilizes Riemannian geometry-based classification [10] and combine it with template matching. Such decoders take covariance matrices obtained from EEG data as features, and therefore they not only capture the univariate spectral power of neural activity from distinct brain regions, but also their multivariate covariance structure. Furthermore, we incorporate an adaptive re-centering step to the detection pipeline [11] to eliminate plausible non-stationarities existing between training and test data sets. We evaluated decoder performance offline on EEG data collected from young, healthy, naïve subjects while performing a task that was designed to evoke both RP and CNV in a sequential manner. Our results show that slow cortical patterns could be detected, verifying the potential of Riemannian geometry-based classification of slow cortical potentials in future BMI applications.

II. METHODS

A. Participants and experimental setup

We recruited 12 young, healthy volunteers without previous experience with BMI systems (mean age: 26.3 ± 4.8 years, all right-handed, 4 females) for this study. The study was approved by the institutional ethics committee (approval number: 2020-03-0073) and all subjects provided written informed consent. Participants were seated in a comfortable armchair in front of a touchscreen computer, where they were asked to perform a center-out reaching task while their EEG was recorded. Electromyographic activity (EMG) of the deltoid and trapezius muscles were also collected by two pairs of bipolar electrodes for movement onset detection purposes.

B. Center-out reach task

Participants awaited trial onset with their right arm resting, approximately 10 centimeters from the touchscreen ('home position'). A trial started by the appearance of a 'home button' at the center of the screen, however subjects were

[1]Department of Neurology, [2]Department of Electrical and Computer Engineering, The University of Texas at Austin, Austin, TX, USA. E-mail: fsr324@austin.utexas.edu, jose.millan@austin.utexas.edu

instructed to wait for 2 seconds before reaching for it, promoting a self-paced movement (RP trials). After touching and holding on the home button, the trial continued either as a 'move' or a 'rest' trial. In the former, following 2 seconds of waiting time —allowing EEG to return to baseline— , two target indicators and a countdown bar appeared on the screen ('prep' cue). When the countdown of 3 seconds finished, targets 'activated' ('go' cue) and participants were instructed to reach and touch one of them as fast as possible (CNV trials). During 'rest' trials, subjects were presented with the same visual interface (although in different color) containing the countdown and targets; however, participants were instructed not to reach for the targets when they activated, but instead to hold on to the home button until the trial was over (no-CNV trials). Finally, subjects also performed 'relax' trials to provide a control condition for RP development, where an inactive home button appeared at the start of the trial and subjects remained relaxed in the home position without reaching for it, until it disappeared after 7 seconds (no-RP trials).

All participants completed 4 runs, each containing 30 'relax' and 30 active trials, with the latter comprised of 15-15 'rest' and 'move' trials. Participants also completed 4 additional runs, each consisting of only 15-15 'rest' and 'move' trials, resulting in a final number of 120 trials for every condition (no-RP, RP, no-CNV, CNV).

C. Data collection and pre-processing

EEG data was collected from 32 standardized cortical locations (International 10-10 system) at 512 Hz with an ANTneuro eego device (ANT Neuro, Netherlands). Raw EEG was band-pass filtered using a 2^{nd} order, zero-phase Butterworth filter with cutoff frequencies 0.1 and 2 Hz and re-referenced to the common average electrode. All following analyses were then performed using data only from a subset of 9 channels (F1, Fz, F2, FC1, FCz, FC2, C1, Cz, C2).

EMG data was collected at 512 Hz from two pairs of bipolar electrodes placed over the deltoid and trapezius muscles. Raw EMG was first high-pass filtered using a 2^{nd} order Butterworth filter with a cutoff frequency of 10 Hz and rectified by taking the absolute value. Then, an additional low-pass filter with cutoff at 100 Hz and a moving average filter with a window size of 0.5 sec was applied to obtain the EMG envelope. Movement onset when reaching for the home button was identified via linear regression as follows. A sliding window of 0.25 second was shifted through EMG data with a one data point step size, and the slope of EMG envelope from both muscles were obtained via ordinary least squares regression. If one of the slopes surpassed a pre-specified threshold in the 1 second preceding pressing of the home button, movement onset was registered. The threshold was set empirically to 0.1 after visual inspection of the data sets.

Pre-processed EEG data was segmented into epochs for all four conditions. For RP trials, 2 seconds of data were selected preceding movement onset as detected by EMG, while from no-RP trials 2 seconds of activity were chosen randomly. For both CNV and no-CNV trials, the entire 3-seconds of data between the 'prep' and 'go' cues were utilized. Finally, trials were rejected from further analysis when either the absolute EEG amplitude surpassed ± 100 μV, or subjects released the home button before targets activated, or subjects did not reach for a target in a 'move' trial (timeout), or subjects erroneously reached for a target in a 'rest' trial.

D. Riemannian geometry-based classification

Riemannian manifolds are smooth manifolds with a finite-dimensional tangent space defined at every point [10]. Covariance matrices obtained from empirical data, being symmetric positive definite (SPD) matrices, lie on the Riemannian manifold [10], [12]. More precisely, let $X \in R^{N_t \times N_{ch}}$ be a band-pass filtered empirical EEG trial data set of N_t data points and N_{ch} channels. Then, the trace normalized sample covariance matrix C is defined as [13]:

$$C = \frac{X^T X}{trace(X^T X)}, \tag{1}$$

where X^T denotes the transpose of X. On a manifold, the shortest distance between two points is called a *gedoesic*. For our current study, we use the following geodesic embedding between two covariance matrices C_i, C_j [14]:

$$\gamma(C_i, C_j, t) = C_i^{\frac{1}{2}} (C_i^{-\frac{1}{2}} C_j C_i^{-\frac{1}{2}})^t C_i^{\frac{1}{2}} \quad t \in [0, 1] \tag{2}$$

Interestingly, the derived Riemannian distance between C_i, C_j using the aforementioned geodesic is invariant to affine transformation on the Riemannian manifold and is known as Affine Invariant Riemannian Metric (AIRM). AIRM allows us to define the Riemannian mean of the set of covariance matrices on the manifold as the point which minimizes the Riemannian distance to individual covariance matrices in the set. Using the AIRM distance and Riemannian mean, a Minimum Distance to Mean (MDM) classifier can be built onto the manifold. MDM is a simple, robust classification method that classifies the covariance matrices directly on the Riemannian manifold based on the AIRM distance to class-specific Riemannian means (see [11] for details on the MDM classification pipeline).

E. Classification pipeline

Classification was carried out offline in a leave-one-run-out cross-validation (CV) scheme, meaning that in every iteration, each trial from a particular run was assigned either to the training or validation sets exclusively. That resulted in a 4-fold CV for RP vs no-RP with a 180/60 train-to-test ratio, while a 8-fold CV for CNV with a 210/30 ratio, as a consequence of the experimental design.

Template matching was incorporated in the model as follows. At each CV iteration, an RP/CNV template was obtained as the average of the corresponding trials in the training set. This template was concatenated to each individual trial in the training set, resulting in epochs of size $N_t \times 2N_{ch}$. Next we estimated the trace normalised covariance of template extended signal using equation 1.

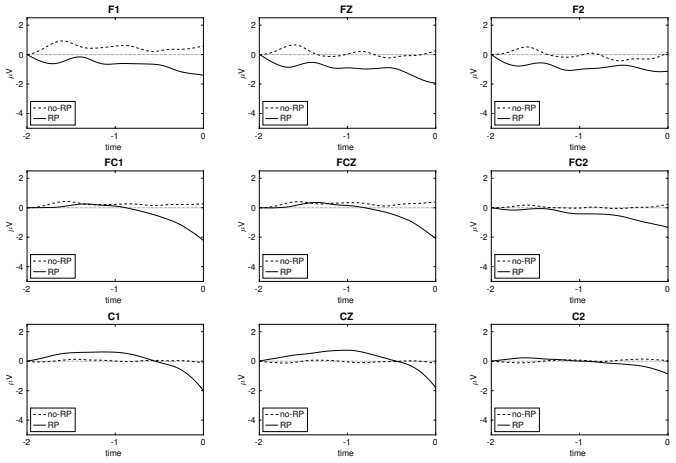

Fig. 1. Grand average Readiness Potentials (RP) at each of the nine electrodes. Data is shown from $t = -2s$ until movement onset ($t = 0$). Dotted line indicates baseline.

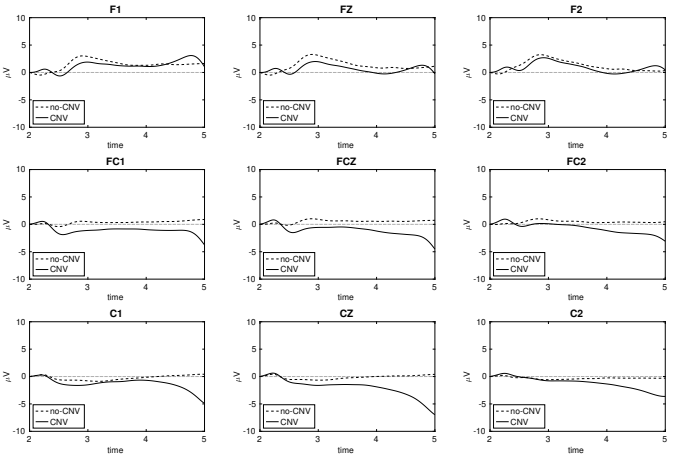

Fig. 2. Grand average Contingent Negative Variation (CNV) at each of the nine electrodes. Data is shown from 'prep' cue ($t = 2$) until 'go' cue ($t = 5$). Dotted line indicates baseline.

Interestingly, the matrices obtained from template-extended data not only capture the covariance structure of the given trial, but also how much it resembles the desired template signal of RP or CNV. Importantly, this 'training' template was concatenated to the trials of the testing set too.

Furthermore, in order to align the distributions of the covariance matrices from training and validation sets, all matrices were re-centered around the identity matrix [11], [15]. As a result, a reference matrix R was obtained as the Riemannian mean of all training trials regardless of class. Then, R was used to re-center all covariance matrices C_i in the training set as [11]:

$$C_i^{rc} = R^{-\frac{1}{2}} C_i R^{-\frac{1}{2}}, \tag{3}$$

where C_i^{rc} is the re-centered version of C_i. Finally, class prototypes to build the MDM classifier for the given CV iteration were obtained as the Riemannian mean of re-centered covariance matrices of each class.

In order to emulate a real-time online RP/CNV detection, incremental recentering was performed to match the distribution of validation trials to the training set before MDM-based classification. Precisely, we followed the order of temporal chronology of validation trials to perform the recentering of the template extended covariance (see [11] for details). The approach was evaluated at the subject level, with independent decoders trained for detecting RP and CNV. Decoder performance was characterized by average accuracy taken over CV iterations. Chance levels were obtained for every subject individually (based on the final number of trials after rejection), assuming a binomial distribution of classification errors [16].

III. Results and Discussion

Figures 1 and 2 show grand average signals for RP and CNV, respectively. A clear buildup of negative potential is observable over the fronto-central and frontal regions of Fig. 1, which is more prominent over regions of the left hemisphere (FC1 and C1). This is not surprising, as all subjects performed the task with their right hand, resulting in an RP dominant in the contralateral hemisphere. On Fig. 2 a roughly symmetric buildup of negative potential is apparent, with highest amplitude over the midline (CZ and FCZ), indicating a CNV. These observations confirm that the task elicited the slow cortical potentials as expected.

TABLE I
Classification accuracies

	RP		CNV	
ID	train	test	train	test
1	78.11%	66.49%	80.09%	76.14%
2	70.88%	62.88%	88.45%	84.17%
3	73.84%	61.60%	83.75%	74.58%
4	70.31%	58.43%	71.55%	65.42%
5	76.59%	67.58%	86.61%	76.18%
6	70.30%	51.12%	79.71%	62.24%
7	78.75%	61.25%	81.13%	69.17%
8	73.70%	62.76%	68.07%	65.57%
9	77.95%	64.45%	92.38%	85.00%
10	79.04%	68.31%	84.35%	79.58%
11	72.57%	60.32%	80.83%	70.42%
12	77.02%	66.48%	86.20%	79.67%
AVG	**74.92%**	**62.64%**	**81.93%**	**74.01%**
STD	**3.37%**	**4.75%**	**6.82%**	**7.49%**
MIN	**70.30%**	**51.12%**	**68.07%**	**62.24%**
MAX	**79.04%**	**68.31%**	**92.38%**	**85.00%**

Classification results are presented in Table I. For RP, average CV test accuracy taken over all subjects was $62.64 \pm 4.75\%$. Nevertheless, except for Subject 6 (51.12%), all accuracies were above chance level. On the other hand, CNV could be detected with an average accuracy of $74.01 \pm 7.49\%$, with all subjects surpassing chance level. Notably, CNV classification accuracy was found the lowest also for Subject 6, raising the possibility of confounding effects with this particular recording (e.g., poor signal quality or lack of subject involvement). With the exclusion of Subject 6, average test accuracies improve to $63.69 \pm 3.22\%$ and $75.08 \pm 6.82\%$ for RP and CNV, respectively.

Clearly, detection of CNV proved to be a less challenging task relative to RP, as indicated by not only higher classification accuracies, but also less model overfitting. The latter is indicated by the fact that the average difference between train and test accuracies was 12.28% for RP while only 7.92% for CNV. This difference in performance might be explained by multiple factors. First, more EEG data were used for CNV detection (3 seconds) when compared to RP (2 seconds). Nevertheless, since development of RP starts roughly at 1-1.5 seconds before movement onset [1], [17], this issue could not be remedied by taking longer epochs. Second, at each iteration the train-to-test ratio for RP was 180/60 compared to that of 210/30 for CNV, resulting in more training data for the latter. Even though it is not a huge difference, with such a small sample size even a small amount of additional training data could substantially affect model fitting. Also, considering this with the more severe overfitting of the decoder, RP detection performances are expected to further improve with more data collection in the future. Third, epochs selected for CNV were well defined in all cases, as the start and end points ('prep' and 'go' cues) were logged by the visual interface. On the other hand, for RP movement onset was detected automatically based on EMG, which itself can introduce errors. Indeed, visual inspection of the data indicated movement onset detection roughly 30-40 ms before a steep rise in EMG envelope in the vast majority of trials. This is hardly surprising as slope estimation was performed prospectively in order to fit an online implementation; i.e., at time t, slope was estimated on EMG data from t to $t + 0.25s$. However, we decided to go with this more conservative approach rather than with other techniques that might identify movement onset with some delay in order for the analyzed epochs containing only preparation but not execution related neural activity. Furthermore, RP has been observed to be vary greatly in morphology depending on a multitude of factors, such as planned force, movement complexity or subjective difficulty [17], which might also affect the data sets analyzed in this study.

Multiple previous studies set out to detect slow cortical potentials on a single-trial basis (e.g., [5], [9], [18], [19]), with many of them utilizing a template matching approach [6], [7], [20]. The technique proposed in our work is not only unique in the sense that no prior efforts applied Riemannian geometry-based classification to RP or CNV detection, but it also combines single-trial analysis and template matching at the same time during the covariance matrix construction. In fact, previous studies have shown that a Riemannian approach seems to be robust to jitters in the latency of EEG potentials [21]. Even though many of the preceding works reported offline detection accuracies surpassing those obtained here, data processing pipelines often included steps that cannot be implemented online, such as spatial filtering using ICA [22], [23] or second-order blind identification [7]. Application of these methods assumes that the identified parameters —such as the ICA mixing matrix— remain stationary over separate sessions for a given subject. Nevertheless, EEG data collected on multiple occasions contain non-stationarities originating from slightly different electrode positions, impedances or changes in the participant's mental states among others [24], therefore the online performance of such methods are expected to deteriorate over time unless tedious regular calibration sessions are introduced. On the other hand, our proposed approach not only can be readily adopted to an online setting without affecting the performance, but the adaptive re-centering step diminishes the effect of non-stationarities and thus promoting consistent performance over multiple sessions [11]. Notably, this re-centering procedure can also be computed online. Furthermore, it has been demonstrated that operating a BMI system is indeed a skill to be learned that requires effort and involvement from the subject side, too [25]–[27], thus a stable decoder performance over sessions of a longitudinal training program is essential for a reliable and robust BMI system. Our method was designed with such considerations in mind, and thus the reported performance measures are expected to further improve when users get to learn to use the application in a series of online sessions.

An obvious limitation of our work is that performance was only evaluated in an offline setting. Therefore, our next goals include testing the Riemannian geometry-based decoder in an online setting, then in a multi-session training program to assess whether users are able to improve their skills in operating the BMI detecting both RP and CNV. Such analyses would pave the way for future online applications of the approach, such as robotic exoskeleton control or motor rehabilitation training programs based on BMI feedback.

IV. Conclusions

Here we propose a novel, Riemannian geometry-based decoding method for detecting slow cortical potentials preceding self-paced and cued movements. Our results show that these neural patterns could be captured with a confidence over chance level, implying potential of the approach for various online BMI applications in the future.

ACKNOWLEDGMENT

This work was partially supported by the Charley Sinclair Fellowship in Neurology.

References

[1] A. Schurger, J. Pak, A. L. Roskies, et al. What is the readiness potential? *Trends in Cognitive Sciences*, 25(7):558–570, 2021.

[2] T. W Kononowicz and T. B. Penney. The contingent negative variation (CNV): Timing isn't everything. *Current Opinion in Behavioral Sciences*, 8:231–237, 2016.

[3] E. Abou Zeid and T. Chau. Electrode fusion for the prediction of self-initiated fine movements from single-trial readiness potentials. *International Journal of Neural Systems*, 25(04):1550014, 2015.

[4] M. Schultze-Kraft, V. Jonany, T. S. Binns, J. Soch, B. Blankertz, and J.-D. Haynes. Suppress me if you can: Neurofeedback of the readiness potential. *Eneuro*, 8(2), 2021.

[5] E. Lew, R. Chavarriaga, S. Silvoni, and J. d. R. Millán. Detection of self-paced reaching movement intention from EEG signals. *Frontiers in Neuroengineering*, 5:13, 2012.

[6] I. K. Niazi, N. Jiang, O. Tiberghien, J. F. Nielsen, K. Dremstrup, and D. Farina. Detection of movement intention from single-trial movement-related cortical potentials. *Journal of Neural Engineering*, 8(6):066009, 2011.

[7] P. Ahmadian, S. Sanei, L. Mussi, L. Ascari, and M. A. Umiltá. Automatic detection of readiness potential. In *9th IASTED International Conference on Biomedical Engineering*, 2012.

[8] M. Mahmoodi, B. M. Abadi, H. Khajepur, and M. H. Harirchian. A robust beamforming approach for early detection of readiness potential with application to brain-computer interface systems. In *39th Annual International Conference of the IEEE Engineering in Medicine and Biology Society*, pages 2980–2983, 2017.

[9] Z. Khaliliardali, R. Chavarriaga, H. Zhang, L. A. Gheorghe, S. Perdikis, and J. d. R. Millán. Real-time detection of driver's movement intention in response to traffic lights. *bioRxiv*, page 443390, 2019.

[10] F. Yger, M. Berar, and F. Lotte. Riemannian approaches in brain-computer interfaces: A review. *IEEE Transactions on Neural Systems and Rehabilitation Engineering*, 25(10):1753–1762, 2016.

[11] S. Kumar, F. Yger, and F. Lotte. Towards adaptive classification using Riemannian geometry approaches in brain-computer interfaces. In *7th International Winter Conference on Brain-Computer Interface*, pages 1–6, 2019.

[12] M. Moakher. A differential geometric approach to the geometric mean of symmetric positive-definite matrices. *SIAM Journal on Matrix Analysis and Applications*, 26(3):735–747, 2005.

[13] H. Ramoser, J. Muller-Gerking, and G. Pfurtscheller. Optimal spatial filtering of single trial EEG during imagined hand movement. *IEEE Transactions on Rehabilitation Engineering*, 8(4):441–446, 2000.

[14] A. Barachant, S. Bonnet, M. Congedo, and C. Jutten. Riemannian geometry applied to BCI classification. In *International Conference on Latent Variable Analysis and Signal Separation*, pages 629–636, 2010.

[15] P. Zanini, M. Congedo, C. Jutten, S. Said, and Y. Berthoumieu. Transfer learning: A Riemannian geometry framework with applications to brain-computer interfaces. *IEEE Transactions on Biomedical Engineering*, 65(5):1107–1116, 2017.

[16] E. Combrisson and K. Jerbi. Exceeding chance level by chance: The caveat of theoretical chance levels in brain signal classification and statistical assessment of decoding accuracy. *Journal of Neuroscience Methods*, 250:126–136, 2015.

[17] H. Shibasaki and M. Hallett. What is the Bereitschaftspotential? *Clinical Neurophysiology*, 117(11):2341–2356, 2006.

[18] G. Gangadhar, R. Chavarriaga, and J. d. R. Millán. Fast recognition of anticipation-related potentials. *IEEE Transactions on Biomedical Engineering*, 56(4):1257–1260, 2008.

[19] D. Liu, W. Chen, K. Lee, R. Chavarriaga, F. Iwane, M. Bouri, Z. Pei, and J. d. R. Millán. EEG-based lower-limb movement onset decoding: Continuous classification and asynchronous detection. *IEEE Transactions on Neural Systems and Rehabilitation Engineering*, 26(8):1626–1635, 2018.

[20] M. Jochumsen and I. K. Niazi. Detection and classification of single-trial movement-related cortical potentials associated with functional lower limb movements. *Journal of Neural Engineering*, 17(3):035009, 2020.

[21] R. Aydarkhanov, M. Uščumlić, R. Chavarriaga, L. Gheorghe, and J. d. R. Millán. Spatial covariance improves BCI performance for late ERPs components with high temporal variability. *Journal of Neural Engineering*, 17(3):036030, 2020.

[22] K. Uto, K. Hibi, and Y. Kosugi. Real-time extraction of readiness-potentials from EEG. In *23rd Annual International Conference of the IEEE Engineering in Medicine and Biology Society*, volume 2, pages 1197–1200, 2001.

[23] F. Karimi, J. Kofman, N. Mrachacz-Kersting, D. Farina, and N. Jiang. Detection of movement related cortical potentials from EEG using constrained ICA for brain-computer interface applications. *Frontiers in Neuroscience*, 11:356, 2017.

[24] H. Raza, H. Cecotti, and G. Prasad. A combination of transductive and inductive learning for handling non-stationarities in motor imagery classification. In *2016 International Joint Conference on Neural Networks*, pages 763–770, 2016.

[25] S. Perdikis, L. Tonin, S. Saeedi, C. Schneider, and J. d. R. Millán. The Cybathlon BCI race: Successful longitudinal mutual learning with two tetraplegic users. *PLoS Biology*, 16(5):e2003787, 2018.

[26] S. Perdikis and J. d. R. Millán. Brain-machine interfaces: A tale of two learners. *IEEE Systems, Man, and Cybernetics Magazine*, 6(3):12–19, 2020.

[27] L. Tonin, S. Perdikis, T. D. Kuzu, J. Pardo, B. Orset, K. Lee, M. Aach, T. A. Schildhauer, R. Martínez-Olivera, and J. d. R. Millán. Learning to control a BMI-driven wheelchair for people with severe tetraplegia. *iScience*, 25(10):1753–1762, 2022.